Stark spectra of Rydberg states in atomic cesium in the vicinity of $n = 18$*

Dong Hui-Jie(董慧杰)[a], Wang Ting(王 婷)[b], Li Chang-Yong(李昌勇)[a]†, Zhao Jian-Ming(赵建明)[a], and Zhang Lin-Jie(张临杰)[a]

[a] State Key Laboratory of Quantum Optics and Quantum Optics Devices, Laser Spectroscopy Laboratory, Shanxi University, Taiyuan 030006, China
[b] College of Physics and Electronics Engineering, Shanxi University, Taiyuan 030006, China

(Received 28 December 2012; revised manuscript received 26 January 2013)

The Stark structures in a cesium atom around $n = 18$ are numerically calculated. The results show that the components of 20D states with a small azimuthal quantum number $|m|$ shift upward a lot, and those with a large $|m|$ shift downward a little within 1100 V/cm. All components of P states shift downward. Experimental work has been performed in ultracold atomic cesium. Atoms initially in $6P_{3/2}$ state are excited to high-n Rydberg states by a polarization light perpendicular to the field, and Stark spectra with $|m| = 1/2, 3/2, 5/2$ are simultaneously observed with a large linewidth for the first time. The observed spectra are analyzed in detail. The relative transition probability is calculated. The experimental results are in good agreement with our numerical computation.

Keywords: Rydberg state, Stark spectrum, ultracold cesium atom, transition probability

PACS: 32.60.+I, 32.30.–r, 67.85.–d **DOI:** 10.1088/1674-1056/22/7/073201

1. Introduction

The Stark effect in Rydberg atoms plays an important role in the fields of quantum control and quantum information. Many relevant theoretical calculations and experimental studies have been reported.[1–11] Silverstone applied a general method of carrying out perturbation theory to any order in an electric field and evaluated the expansion through the twenty-fifth order for hydrogen atoms.[12] Tian proposed a new method of calculating the exact complex eigenvalues of Schrodinger equations for a hydrogen atom in a uniform electric field.[13] Zhi *et al.* made a comprehensive study on the Stark structures of the Rydberg states of alkaline-earth atoms.[14] Shen *et al.* used the Stark effect to determine a more accurate Eu atom ionization threshold.[15] Zimmerman and co-workers calculated the Stark structures of alkali metal atoms in the vicinity of $n = 15$, and introduced the calculation method in detail.[16] They also experimentally observed the Stark spectra of Li ($|m| = 0, 1$) and Cs ($|m| = 1/2$) in the vicinity of $n = 15$. Hu *et al.* used the molecular beam technique to study the Stark spectra and energies of cesium Rydberg states with $n = 21, 22, 23$ in the electric field intensity range of $0 - 600$ V/cm.[17] Singer *et al.* studied the Stark structure and spectra of rubidium atoms in the vicinity of $n = 79, 80$.[18] In most of these studies, the atoms in the ground state are first excited to S states through a two-photon process, then further excited to higher states by a polarized light parallel or perpendicular to the field. The final states of $m = 0$ or $|m| = 1$ are populated, respectively. Considering the fine structure, the final states which are pumped from $S_{1/2}$ state will be $|m| = 1/2$ or $|m| = 1/2, 3/2$ states, respectively. In a more general method, atoms are first excited to S, P, D, F states, and so on, then re-excited to high Rydberg states, and thus more $|m|$ states should be observed simultaneously due to the selection rule $\Delta m = \pm 1$. In this article, the ultracold cesium atoms are prepared in a magneto-optical trap (MOT) with a static electric field. The atoms in the ground states are excited to $6P_{3/2}$ states by trapping or repumping lasers. Then, a pulsed dye laser polarized perpendicularly to the field is used to excite atoms to higher Rydberg states. We obtain a mixture of $|m| = 1/2, 3/2, 5/2$ Stark spectra around $n = 18$. We also perform the corresponding theoretical computation. The Stark structures are analyzed in detail. The reason for energy-level anti-crossing is revealed. Our calculated results of transition probability are in good agreement with observed ones of spectral intensity.

2. Experimental procedure

A schematic diagram of the experimental arrangement for cesium is shown in Fig. 1. More details about the experimental system have been addressed in our former papers.[19–22] Here, we just give a brief introduction.

The sample of cesium is cooled and trapped in a conventional vapor cell MOT. The trapping and repumping lights are provided by two diode lasers (Toptica DL100), which have an output wavelength of 852 nm. The trapping laser is red-detuned by about three natural linewidths of the atomic

*Project supported by the National Basic Research Program of China (Grant No. 2012CB921603), the National Natural Science Foundation of China (Grant Nos. 61078001, 61178009, 11274209, and 60778008), the Fund for Fostering Talents in Basic Science of the National Natural Science Foundation of China (Grant No. J1103210), the Natural Science Foundation of Shanxi Province, China (Grant No. 2012011003-2), and the Shanxi International Collaboration Program (Grant No. 2010081046).

†Corresponding author. E-mail: lichyong@sxu.edu.cn

© 2013 Chinese Physical Society and IOP Publishing Ltd

transition $6S_{1/2}(F=4) \rightarrow 6P_{3/2}(F'=5)$ by an acousto-optical modulator (AOM). The repumping laser is locked to the $6S_{1/2}(F=3) \rightarrow 6P_{3/2}(F'=4)$ atomic transition to make sure the population in the $6S_{1/2}(F=3)$ level returns to the $6S_{1/2}(F=4)$ level. The cold atom cloud is prepared in the midway between two parallel metal grids with a 15-mm distance.

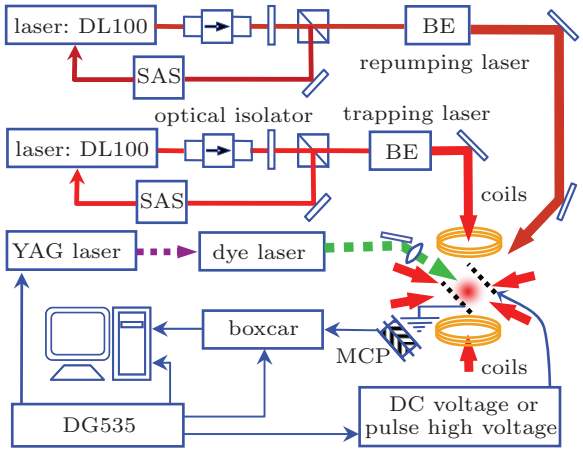


Fig. 1. (color online) Experimental setup. SAS: saturation absorption spectrum; BE: beam expander; MOT: magneto-optical trap; MCP: microchannel plate.

The ultracold Rydberg atoms are produced by two-photon excitation. The first photon emitting from the trapping or repumping laser, excites the ultracold neutral atoms in the ground state up to $6P_{3/2}$ state. At the field strength lower than 2000 V/cm, the Stark effect for the $6P_{3/2}$ state can be ignored. Our calculated Stark shift of $6P_{3/2}$ ($|m|=1/2$) energy level at field intensity of 2000 V/cm is just -3.0×10^{-6} cm^{-1} or -90 kHz. The negative sign means a red shift or drop. It is much less than the linewidth of the pulse dye laser (Spectra-Physics PDL-3), namely, 0.2 cm^{-1}. Hence, the Stark effect for the low-n states is not taken into account. The dye laser is used as a light source of the second-step excitation, and is pumped by a frequency-tripled pulsed Nd:YAG laser (Spectra-Physics DCR-2). Its output pulse is 7 ns in duration, running at a repetition rate of 10 Hz. Its wavelength is tunable from 480 to 540 nm with LDS 510 dye. A wavemeter (HighFinesse/Angstrom, WS-7R) with an accuracy of 0.002 cm^{-1} is used to calibrate the wavelengths of the dye laser. A static field provided by a well-regulated high-voltage supply (Bertan 230) whose amplitude is variable, is applied to the two grids. Due to the interaction with the external field, atomic levels are split and shifted. By scanning the dye laser frequency, the atoms would be populated to the Stark levels of high-n Rydberg states as the energy is resonant. The dye laser output energy is about 1.5 mJ at 510 nm, which is so intense that it can provide surplus photons to ionize the atoms in the resonant Stark levels. This is called resonantly enhanced multi-photon ionization (REMPI) spectroscopy. The zero-field Rydberg atom signal is produced by pulsed field ionization. The pulsed field amplitude is 2000 V/cm with 25-ns rising time and 10-μs duration. The ions are accelerated by the static electric field or the pulsed field, and fly to a dual-stacked micro channel plate (MCP) detector. The amplified ion signals are fed to a boxcar integrator averager (SRS-250), then read and stored by a personal computer for further analysis. The digital delay/pulse generator (SRS DG535) is used to control the time sequence of dye laser, pulse electric field, Boxcar, oscilloscope, and data collecting.

3. Numerical calculations

The numerical method has been introduced in our former papers.[23,24] It is similar to that used in Ref. [16]. Several differences are presented as follows.

(i) We use the latest experimental energy data of the atomic cesium and the energy formula $E=-R/[2(n-\delta_{n,l,j})]$ to calculate the radial wavefunction, and further the radial-matrix elements. Here, R is the Rydberg constant for atomic cesium and equals 109736.86224 cm^{-1}.[25] The quantum defect is expressed by the extended Rydberg–Rietz formula in the form of

$$\delta_{n,j,l} = a+\frac{b}{(n-a)^2}+\frac{c}{(n-a)^4} + \frac{d}{(n-a)^6}+\frac{e}{(n-a)^8}+\cdots, \quad (1)$$

where the values of coefficients a, b, c, d, and e are listed in Table 1.

(ii) The matrix element integer is performed in the inward direction because only the outer boundary condition is known. The starting point r_1 is determined by $2n(n+15)$, where the value of the radial wavefunction is $X_1=0$. The second point is calculated by $X_2=(-1)^{(n-l+1)}\times10^{-10}$. The sign of X_2 is the same as that of the analyzed wavefunction of hydrogen, so that they have an identical phase at infinity. The calculated step is taken to be 0.01. According to the Numberov algorithm, the third point can be calculated based on the first two points. The calculation of the radial wave function will terminate when it begins to diverge or oscillate faster than the integration grid size.

(iii) We solve the following matrix equation to obtain the Stark energy eigenvalue E_i:[5]

$$\begin{pmatrix} E_1^0+H_{11}^{\rm s} & \cdots & H_{1N}^{\rm s} \\ \vdots & \ddots & \vdots \\ H_{N1}^{\rm s} & \cdots & E_N^0+H_{NN}^{\rm s} \end{pmatrix} \begin{pmatrix} a_{i1} \\ \vdots \\ a_{iN} \end{pmatrix} = E_i \begin{pmatrix} a_{i1} \\ \vdots \\ a_{iN} \end{pmatrix}. \quad (2)$$

Here, $H_{ij}^{\rm s}=\langle\varphi_i|H^{\rm s}|\varphi_j\rangle$ is the matrix element of the unperturbed states with the perturbation operator, $E_i^0+H_{ii}^{\rm s}$ is the diagonal element, $H_{ii}^{\rm s}=0$ because it includes the factor $\delta(l,l'\pm1)$,[16] E_i^o is the zero-field energy of Rydberg states, and a_{ij} are the coefficients of terms of the wavefunction with external field.

Table 1. Coefficients of the extended Rydberg–Rietz formula for Cs I.

	a	*b*	*c*	*d*	*e*	*f*
$n^2S_{1/2}$ [a]	4.04935665(38)	0.2377037	0.255401	0.00378	0.25486	–
$n^2P_{1/2}$ [a]	3.59158950(58)	0.360926	0.41905	0.64388	1.45035	–
$n^2P_{3/2}$ [b]	3.559058	0.374	–	–	–	–
$n^2D_{3/2}$ [b]	2.475365	0.5554	–	–	–	–
$n^2D_{5/2}$ [a]	2.46631524(63)	0.013577	−0.37457	−2.1867	−1.5532	−56.6739
$n^2F_{5/2}$ [a]	0.03341424(96)	−0.198674	0.28953	−0.2601	–	–
$n^2F_{7/2}$ [b]	0.033537	0.191	–	–	–	–
$n^2G_{7/2}$ [a]	0.00703865(70)	−0.049252	0.01291	–	–	–

[a] Ref. [25], [b] Ref. [26].

In order to interpret observed Stark spectra, we also calculate the transition probability. The transition probability from $6P_{3/2}$ to high-n Stark states is calculated by

$$f = \frac{2}{3}(E' - E)|\langle El\,jm|\boldsymbol{F}\cdot\boldsymbol{r}|E'l'\,j'm\rangle|^2, \tag{3}$$

where $\langle El\,jm|$ is the wavefunction of $6P_{3/2}$ state, $\langle E'l'\,j'm'|$ is the wavefunction of high-n Stark states, E and E' are the state energies, $\boldsymbol{F}$ is the external electric field, and $\boldsymbol{r}$ is the radial coordinate.

4. Results and discussion

4.1. Theoretical results and discussion

The theoretical results of Stark structures for $|m| = 1/2$, 3/2, and 5/2 around $n = 18$, together with experimental spectra, are shown in Fig. 2. From calculated curves we know that the levels with the same $|m|$ anti-cross with each other, and ones with different $|m|$ cross. This is very universal and obeys relative theorem. As an example, $20D_{5/2}$ ($|m| = 5/2$) level crosses with $20D_{3/2}$ ($|m| = 1/2$) level at about 150 V/cm. These two components with other principle quantum numbers also cross, just like that shown in latter figures. The calculated results indicate that $|m| = 1/2, 3/2$ components of the $20D_{5/2}$ level have a small interval between them, and they all move upward a lot. The $|m| = 5/2$ components shift downward a little within 1100 V/cm. The other D states are similar to 20D states. Thus, we conclude that for D states, $|m| = 1/2, 3/2$ components move upward a lot, and $|m| = 5/2$ components shift downward a little within a certain electric field. The case of P states is not the same as that of D states. The components of P states always shift downward within a certain field.

Because quantum defects of 22S, 18F, and 18G states are close to an integer (see Table 1, column 2, $\delta_S \simeq 4.049$, $\delta_F \simeq 0.033$, $\delta_G \simeq 0.007$), they are very close to the $n = 18$ manifold states. In the external field, the 22S state almost crosses with the $|m| = 1/2$ components of 18F states, and the latter almost crosses with the components of 18G state. As to the components of 18G states, because of smaller quantum defect of $\delta_G \simeq 0.007$, they cannot be distinguished from the $n = 18$ manifold states (Fig. 2). This indicates that the interval or anti-crossing between neighbor components is caused by quantum defect. We know that a hydrogen atom has no quantum defect, or we can say that it has an integer quantum defect of 0. Therefore, its Stark levels cross no matter what $|m|$ is. In order to study the quantum defect effect on the neighboring Stark levels, we postulate that the S states in a hydrogen atom have a quantum defect δ_S, and other states have

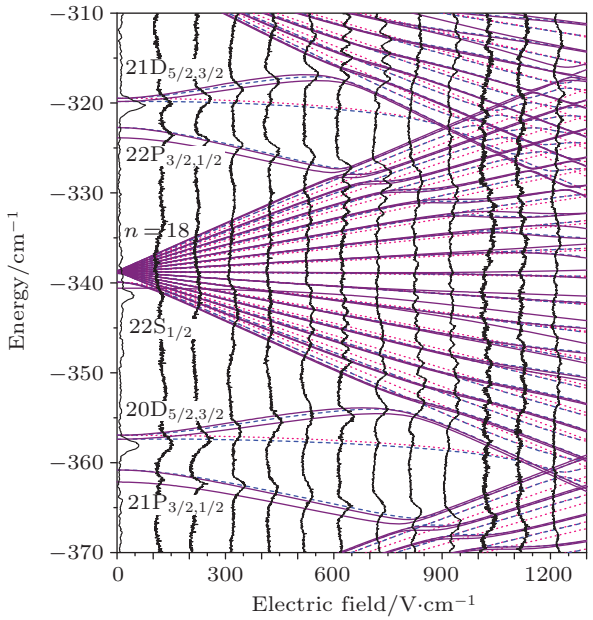


Fig. 2. (color online) Calculated and experimental Stark structures of atomic cesium around $n = 18$. Solid, dashed, and dotted lines correspond to $|m| = 1/2, 3/2, 5/2$ levels, respectively.

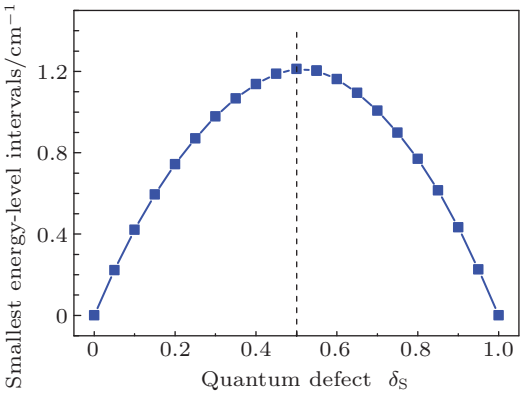


Fig. 3. (color online) Stark level separations between ($n = 18$, $n_1 = 0$, $m = 0$) and ($n = 17$, $n_1 = 16$, $m = 0$) versus quantum defect δ_S for the S states in an atomic hydrogen.

no change. Then, we calculate the Stark level intervals between $(n=18, n_1=0, m=0)$ and $(n=17, n_1=16, m=0)$ with various quantum defect δ_S. Here, n_1 is the parabolic quantum number,[27] which is a non-negative integer. The curve of the separation versus δ_S is shown in Fig. 3. It is evident that the interval vanishes as $\delta_S \to 0$ or $\delta_S \to 1$. Thus, we can conclude that non-integer quantum defects cause the Stark energy level's anti-crossing.

4.2. Experimental results and discussion

We also experimentally observe the spectra of zero-field cesium Rydberg states with field ionization technology by scanning the dye laser wavelength. The atoms are excited to high-n Rydberg states from the $6P_{3/2}$ state, so nS and nD states are optically allowed states according to the dipole transition selection rules. With a different external field, the Stark structures are obtained by scanning the final laser frequency while monitoring the Rydberg state population by the REMPI spectroscopy. The polarization direction of the final laser is perpendicular to the field, so we obtain the spectra including $|m| = 1/2, 3/2, 5/2$ Stark states in every scanning process. Figure 2 shows the experimental results around $n = 18$ together with the theoretical ones as a comparison. From Fig. 2, we know several points as follows.

(i) In zero field, we can only observe S and D Rydberg states, but the transitions from the components of other states in static field are observed. This is because that the zero-field selection rule $\Delta l = \pm 1$ is not appropriate and replaced by $\Delta m = 0, \pm 1$. For example, in the electric field, the high-n P state component has a strong intensity and a wider linewidth (Fig. 2), but its intensity is equal to zero at zero field.

(ii) Within experimental wavelength range, the pulsed dye laser linewidth is about 0.2 cm^{-1}. The state components with different $|m|$ slightly split, and they cannot be distinguished in the spectra. However, this induces wider linewidth, such as D and P states in Fig. 2. The linewidths for 20D and 21D states in external field are about two times larger than that without field.

(iii) From Fig. 2, we also know that the manifold levels are only partly observed. This is similar to the case of $n = 15$.[16] They are determined by the transition probability.

(iv) In Fig. 2, nD and nP components cannot be distinguished because of the small energy interval between them and large dye laser line-width. In order to experimentally distinguish between different components, we measure the Stark spectra of low-n D and P states. Figure 4 shows the Stark spectra of 15D and 16P states, and figure 5 shows those of 14D and 15P. From these two figures, we know that the $j = 3/2$ states for P and D states have a great feature, but the other j states are so weak that they cannot be identified in the spectra. Specifically, there is no spectrum arising from $15P_{1/2}$ and $16P_{1/2}$ states. In order to explain this experimental result, we calculate the transition probability from $6P_{3/2}$ to $16P_{3/2,1/2}$ at various electric fields (Fig. 6). The transition from $6P_{3/2}$ to $16P_{3/2}$ is gradually enhanced with increasing field intensity. The transition probability from $6P_{3/2}$ state to $16P_{1/2}$ ($|m| = 1/2$) state almost equals zero at the field intensities of less than 600 V/cm. In the range above 600 V/cm, the transition probability increases with the field relatively slowly. Therefore, we observed no spectrum from $16P_{1/2}$ ($|m| = 1/2$) state. Figures 2 and 4–6 show that our theoretical calculations are in good agreement with the experimental results. The experimental error is mainly due to wider linewidth of dye laser. The theoretical calculation also causes a slightly bigger error for heavy atoms than for light ones.[24,25]

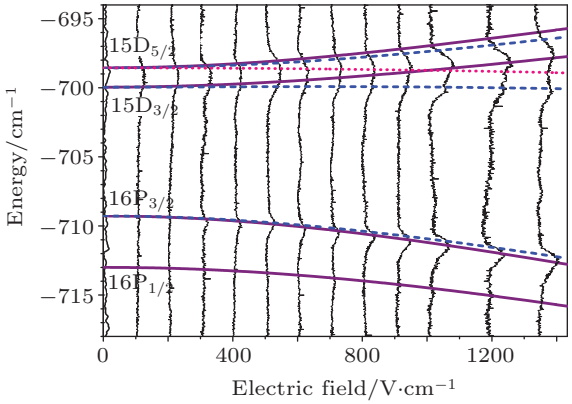


Fig. 4. (color online) Calculated Stark structures and observed spectra of cesium atom in the vicinity of 15D and 16P. Solid, dashed, and dotted lines are associated with $|m| = 1/2, 3/2, 5/2$, respectively.

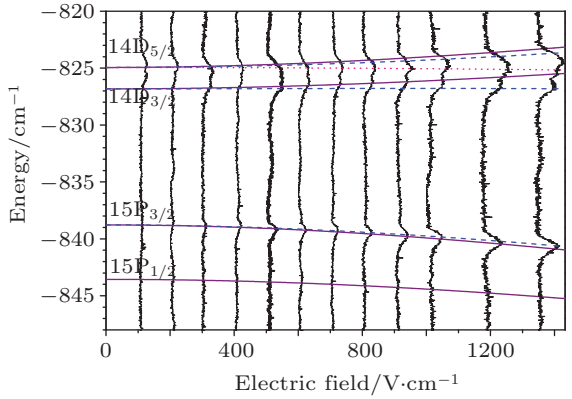


Fig. 5. (color online) Calculated Stark structures and observed spectra of cesium atom in the vicinity of 14D and 15P. Solid, dashed, and dotted lines represent calculated levels of $|m| = 1/2, 3/2, 5/2$, respectively.

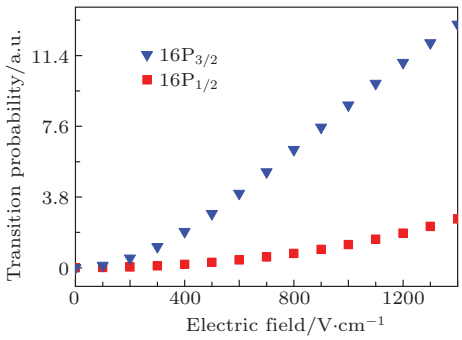


Fig. 6. (color online) The transition probability from $6P_{3/2}$ to $16P_{3/2,1/2}$ versus the electric field.

5. Conclusions

The Stark structures of atomic cesium in the vicinity of $n = 18$ have been numerically computed. The components of $n\mathrm{D}_{5/2}$ ($|m| = 1/2, 3/2$) states with a small separation move upward a lot. The components of $|m| = 5/2$ shift downward a little within a certain range of electric field. The components of nP states always shift downward within a certain field range. Because quantum defects of S and F states are very close to an integer, the components of these states have a small separation with other neighboring components. This indicates that the separation vanishes as the quantum defect δ is integer. The cesium Stark spectra in the vicinity of $n = 18$ are obtained by the REMPI spectroscopy in an ultracold atomic cesium. The signals of $n\mathrm{P}_{3/2}$ state are obvious in the external field, which cannot be observed at a zero field with the current exciting mechanism. The components of $15\mathrm{P}_{1/2}$ and $16\mathrm{P}_{1/2}$ states have no feature in spectra within the field of 1400 V/cm. This is explained in terms of our calculated transition probability. The computed results are in good agreement with our experimental ones.

References

[1] Bethlem H L and Meijer G 2003 *Int. Rev. Phys. Chem.* **22** 73
[2] Vliegen E, Hogan S D, Schmutz H and Merkt F 2007 *Phys. Rev. A* **76** 023405
[3] Bichsel B J, Morrison M A, Shafer-Ray N and Abraham E R I 2007 *Phys. Rev. A* **75** 023410
[4] Gavrilenko V P, Kim H J, Ikutake T, Kim J B, Choi Y W, Bowden M D and Muraoka K 2000 *Phys. Rev. E* **62** 7201
[5] Kampschulte T, Schulze J, Luggenholscher D, Bowden M D and Czarnetzki U 2007 *New J. Phys.* **9** 18
[6] Jiang T, Bowden M D, Wagenaars E, Stoffels E and Kroesen G M W 2006 *New J. Phys.* **8** 202
[7] Czarnetzki U, Luggenholscher D and Dobele H F 1998 *Phys. Rev. Lett.* **81** 4592
[8] Ritter S, Gartner P, Baer N and Jahnke F 2007 *Phys. Rev. B* **76** 165302
[9] Pisharody S N, Zeibel J G and Jones R R 2000 *Phys. Rev. A* **61** 063405
[10] Kulina P and Rinkleff R H 1985 *J. Phys. B* **18** L245
[11] Zhu X B, Zhang H, Feng Z G, Zhang L J, Li C Y, Zhao J M and Jia S T 2010 *Acta Phys. Sin.* **59** 2401 (in Chinese)
[12] Silverstone H J 1978 *Phys. Rev. A* **18** 1853
[13] Tian R H 2003 *Chin. Phys. Lett.* **20** 493
[14] Zhi M C, Dai C J and Li S B 2001 *Chin. Phys.* **10** 929
[15] Sheng L, Ye S W and Dai C J 2012 *Acta Phys. Sin.* **61** 063301 (in Chinese)
[16] Zimmerman M L, Littman M G, Kash M M and Kleppner D 1979 *Phys. Rev. A* **20** 2251
[17] Hu Z F, Zhao H T, Zhou S K, Gong S S and Shan M S 2000 *Chin. Phys.* **9** 805
[18] Singer K, Reetz-Lamour M, Amthor T, Folling S, Tscherneck M and Weidemuller M 2005 *J. Phys. B* **38** S321
[19] Zhao J M, Zhang H, Feng Z G, Zhu X B, Zhang L J, Li C Y and Jia S T 2011 *J. Phys. Soc. Jpn.* **80** 034303
[20] Zhang H, Che J L, Feng Z G, Zhang L J, Zhao J M and Jia S T 2011 *J. Phys. Soc. Jpn.* **80** 104301
[21] Feng Z G, Zhang H, Zhang L J, Li C Y, Zhao J M and Jia S T 2011 *Acta Phys. Sin.* **60** 073202 (in Chinese)
[22] Che J L, Zhang H, Feng Z G, Zhang L J, Zhao J M and Jia S T 2012 *Acta Phys. Sin.* **61** 043205 (in Chinese)
[23] Li C Y, Hao T, Zhang H, Zhu X B, Tao G Q, Zhang L J, Zhao J M and Jia S T 2012 *J. Phys. Soc. Jpn.* **81** 044302
[24] Li C Y, Zhang H, Zhao J M and Jia S T 2012 *Acta Phys. Sin.* **61** 163202 (in Chinese)
[25] Weber K H and Sansonetti C J 1987 *Phys. Rev. A* **35** 4650
[26] Goy P, Raimond J M, Vitrant G and Haroche S 1982 *Phys. Rev. A* **26** 2733
[27] Gallagher T F 1994 *Rydberg Atoms* (New York: Cambridge University Press) p. 72